

# A Novel Hosting Capacity Evaluation Method for Distributed PV Connected in Power System Based on Maximum Likelihood Estimation of Harmonic

Hongtao Shi, Jiahao Zhu<sup>✉</sup>, Yuchao Li<sup>✉</sup>, Zhenyang Yan, Tingting Chen, and Bai Zhang

**Abstract**—Methods for fully characterizing the harmonic injection amount of distributed photovoltaic grid connection and combining harmonic constraints with other constraints to accurately evaluate the hosting capacity of photovoltaic integration into distribution networks are of great significance as they ensure the safe and stable operation of distribution networks. Therefore, a novel hosting capacity evaluation method for distributed photovoltaics (PVs) connected in a power system based on the maximum likelihood estimation of harmonics (MLE) is proposed in this study. First, using the likelihood function from the MLE method, the harmonic parameters of distributed photovoltaic injections are optimally estimated, allowing for the accurate assessment of harmonic outputs during photovoltaic grid connections. Furthermore, a harmonic partitioning method is devised; it characterizes the connection degree between nodes in the grid-connected system, and it divides the distribution network into regions. The scenario number in the estimation of hosting capacities is effectively reduced. Finally, a comparison is carried out relative to the conventional hosting capacity. The assessment method proposed in this study considers the harmonic access in the actual distributed PV grid-connected system. An improved harmonic partitioning method is established based on the harmonic injection amount. The evaluation of PV hosting capacities in the region ensures accuracy and reduces calculation times. They provide references for the access capacity of the distribution network.

**Index Terms**—Maximum likelihood estimation (MLE), hosting capacity assessment, harmonic, partition of distribution network.

## I. INTRODUCTION

PHTOTOVOLTAIC power generation technology has been extensively researched and applied. With a high percentage of distributed photovoltaic (PV) integrated into the distribution grid, the operational status of the distribution grid has changed considerably. There may be phenomena, such as out-of-limit voltage, line overload, power reverse transmission, and harmonic distortion, which introduce negative effects with respect

Received 20 September 2024; revised 5 November 2024 and 22 December 2024; accepted 3 February 2025. Date of publication 26 February 2025; date of current version 21 April 2025. This work was supported in part by the National Natural Science Foundation of China under Grant 52267013 and in part by the Key Research and Development Program of Ningxia under Grant 2022BEE03004. (*Corresponding author: Jiahao Zhu*)

The authors are with the School of Electrical and Information Engineering, North Minzu University, Yinchuan 750021, China (e-mail: peneg@sina.com; owlxiogui@163.com; liyuchao0318@163.com; 13469743787@163.com; ctt07072022@163.com; zhangbai6402@163.com).

Digital Object Identifier 10.1109/JPHOTOV.2025.3541402

to the safety and stability of the power grid [1]. Therefore, finding the limiting factors of PV access capacities and determining the maximum capacity of PV grid connections are indispensable for the planning and optimal operation of distribution networks and new energy sources [2].

Currently, the constraints on the grid-connected hosting capacity of distributed power sources mainly focus on the following aspects. On the one hand, traditional single-constraint conditions, such as out-of-limit voltage, are used as the limiting factors of hosting capacity. Combined with the objective function of minimizing active power loss, the photovoltaic access capacity of the distribution network is determined [3], [4]. Under the condition that the system's voltage deviation and voltage fluctuation do not exceed the limit, the limit capacity of the distribution network is analyzed. Furthermore, starting with the risk assessment index of voltage limits, the hosting capacity of the distribution network is effectively evaluated [5], [6]. On the other hand, multiple constraints, such as voltage and line current, are used as limiting factors for distribution network hosting capacities in assessments with multiple types of constraints; then, the minimum active power loss is taken as the objective function to analyze the hosting capacity of distribution networks from various perspectives [7], [8], [9]. Furthermore, the distribution of harmonics under different power penetration rates is quantitatively analyzed through calculations of multiple power access scenarios, providing a reference for reducing harmonic content [10]. However, there are still shortcomings in the research on the harmonic content of distributed power generation grid connections, and the harmonic constraint model is not sufficiently refined, resulting in the inaccurate evaluations of hosting capacities. Moreover, a high proportion of photovoltaics and a large number of constraints result in the inaccurate assessment of carrying capacities and long assessment times. Consequently, when determining the hosting capacity of the distribution network, the optimal solution is typically obtained by considering various safety constraints and applying different optimization algorithms [11]. Currently, optimization methods, such as intelligent optimization and random scenario simulation, are generally used. While the evaluation process is simple and intuitive, the main disadvantage is the large computational demand.

Therefore, a novel hosting capacity evaluation method for distributed PVs connected in power systems based on the maximum likelihood estimation of harmonics (MLE-harmonic)

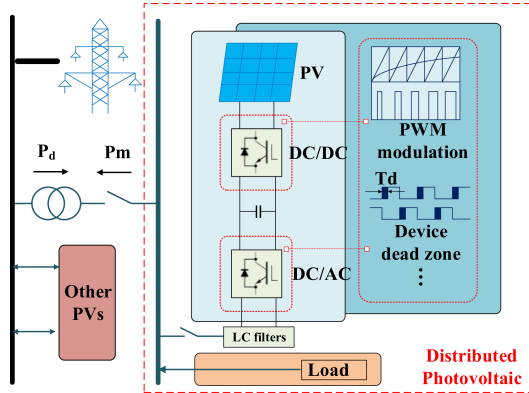


Fig. 1. Schematic diagram of distributed PV structure.

is proposed in this article. The MLE is used to accurately describe the harmonics injected by the grid-connected distributed photovoltaic system, and a new harmonic constraint model is constructed for the hosting capacity evaluation. The ability to consider multiple types of constraints in a coordinated and integrated manner reflects the true hosting capacity. Furthermore, the coupling relationship of each node in the distribution network under the influence of harmonic injection is characterized using the improved harmonic electrical distance. A harmonic partitioning method is constructed, which divides the PV access area. This method reduces the computation time per region while maintaining accuracy with respect to photovoltaic capacity access, thereby solving numerous problematic scenarios and the long computation times associated with traditional distributed photovoltaic access and improving the accuracy of hosting capacity evaluation.

## II. HOSTING CAPACITY FOR DISTRIBUTED PVs CONNECTED IN POWER SYSTEMS

### A. Structure and Principle of Distributed Photovoltaic Grid Connections

Distributed PVs comprise four parts: photovoltaic cells, inverters, controllers, and filters [12]; these are shown in Fig. 1.

In Fig. 1, the high-order harmonics generated via pulsewidth modulation and the low-order harmonics caused by the device's deadband effect are the main sources of current and voltage distortions [13], [14]. They cause a large amount of harmonics to enter the distribution network, which, in turn, results in harmonic pollution in the distribution network and may affect hosting capacities. Therefore, it is necessary to assess the amount of harmonics injected via PV.

### B. Hosting Capacity Assessment for Distributed Photovoltaic Grid Connections

The maximum hosting capacity of the distribution network node is taken as the objective function [15]

$$F_{DN} = \max P_{PV} \quad (1)$$

where  $F_{DN}$  is the objective function, and  $P_{PV}$  is the total active power output from the distributed PV grid connection.

Furthermore, the hosting capacity of PV grid connections needs to satisfy multiple constraints, such as power flow constraints, current constraints, and harmonic constraints.

Regarding harmonic constraints, harmonic power flow calculations are adopted to analyze the influence of harmonics on each node of the distribution network [16]. The harmonic distortion rate is determined via the ratio of harmonic current to fundamental current [17]. Simultaneously, the harmonic power flow is used to determine the harmonic voltage at each node through the harmonic bus admittance matrix, thus obtaining the system's harmonic distortion rate.

Assuming that the number of nodes in the grid-connected system is  $M$ , the harmonic admittance matrix  $Y_{h(M)}$  is determined according to the harmonic parameters and branch connections of distributed PV into the distribution network. The formula is given as follows [18]:

$$Y_{h(M)} = \begin{bmatrix} Y_{h(1,1)} & Y_{h(1,2)} & \cdots & Y_{h(1,j)} \\ Y_{h(2,1)} & Y_{h(2,2)} & \cdots & Y_{h(2,j)} \\ \vdots & \vdots & \ddots & \vdots \\ Y_{h(i,1)} & Y_{h(i,2)} & \cdots & Y_{h(i,j)} \end{bmatrix}_{M \times M} \quad (2)$$

where  $h$  is the number of harmonics of the distributed PV grid connection;  $M$  is the total number of nodes,  $i$  and  $j$  are the nodes of the grid-connected system; and  $h(i, j)$  represents the node connection relationship under the harmonic number;  $i = 1, 2, \dots, M$  and  $j = 1, 2, \dots, M$ .

For the  $h$ th harmonic, there is the following harmonic power flow node voltage equation:

$$I_{h(i)} = Y_{h(M)} U_{h(i)} \quad (3)$$

where  $I_{h(i)}$  is the current vector injected by the harmonics at node  $i$ ; and  $U_{h(i)}$  is the voltage vector injected by the harmonics.

The harmonic ratio and total harmonic distortion are shown in the following formula [19]:

$$\text{HRU}_{h(i)} = \frac{U_{h(i)}}{U_{1(i)}} \times 100\% \quad (4)$$

$$\text{THD}_{h(i)} = \frac{\sqrt{\sum_{h=2}^{\infty} (U_{h(i)})^2}}{U_{1(i)}} \times 100\% \quad (5)$$

where  $\text{HRU}_{h(i)}$  is the harmonic ratio at node  $i$ ,  $\text{THD}_{h(i)}$  is the total harmonic distortion at node  $i$ , and  $U_{1(i)}$  is the fundamental voltage of node  $i$ .

Furthermore, the capacity for the distributed network with PV is affected by the size of the harmonic distortion rate. It is necessary to set the voltage distortion rate constraint to study the maximum capacity that the distribution network can access. The formula is given as follows:

$$\text{THD}_{h,PV} = \frac{\sqrt{\sum_{h=2}^{\infty} (U_{h,PV})^2}}{U_{1,PV}} \times 100\% < \text{THD}_{h,PV \max} \quad (6)$$

where  $h$  is the number of harmonics,  $\text{THD}_{h,PV}$  is the  $h$ th harmonic voltage distortion rate,  $U_{h,PV}$  is the  $h$ th harmonic voltage,  $U_{1,PV}$  is the initial fundamental voltage, and  $\text{THD}_{h,PV \max}$  is the total harmonic voltage distortion rate under the national

standard. The influence of the photovoltaic grid-connected system on the harmonics needs to meet the limits of the harmonic voltage-containing rate and total harmonic distortion rate in the standard.

### III. HOSTING CAPACITY EVALUATION METHOD FOR DISTRIBUTED PVs CONNECTED IN POWER SYSTEMS BASED ON THE MLE-HARMONICS

#### A. MLE-Harmonic

MLE is a method for evaluating system parameters, given observational data and a probability model [20]. The random fluctuation characteristics of harmonic current amplitude can be described by a normal distribution [21]. The process of constructing a harmonic maximum likelihood estimate is specified as follows.

Since the harmonic sample sets generated by distributed PV are randomly selected mutually independent samples, only one harmonic amplitude sample set can be considered. The formula is given as follows:

$$H_x = \{I_{(x)1}, I_{(x)2}, I_{(x)3}, \dots, I_{(x)n}\} \quad (7)$$

where  $H_x$  is the harmonic amplitude sample,  $I_x$  is the amplitude of the collected harmonic current, and  $n$  is the number of samples collected. The likelihood function  $l(\theta_x|H_x)$  of the system is described using the following equation [22]:

$$\begin{aligned} l(\theta_x|H_x) &= p(H_x|\theta_x) = \prod_{i=1}^n p(I_{(x)i}; \theta_x) \\ &= p(I_{(x)1}, I_{(x)2}, I_{(x)3}, \dots, I_{(x)n}|\theta_x) \end{aligned} \quad (8)$$

where  $\theta_x$  is the parameter vector of harmonics,  $P(H_x|\theta_x)$  is the joint density function of the harmonics,  $p$  is the probability, and  $I_{(x)i}$  is each harmonic sample value,  $i = 1, 2, \dots, n$ .

Furthermore, the derivation of  $\theta_x$  in formula (8) is carried out, as shown in the following equation:

$$\hat{\theta} = \frac{d(l(\theta_x|H_x))}{d\theta_x} = \frac{d \prod_{i=1}^n p(I_{(x)i}; \theta_x)}{d\theta_x} \quad (9)$$

where  $\hat{\theta}$  is the maximum likelihood estimator of  $\theta_x$ . From the above, it can be observed that the harmonic amplitude dataset approximately obeys a normal distribution, and its harmonic maximum likelihood function is shown as follows [23]:

$$L(\mu_x, \sigma_x^2|H_x) = \prod_{i=1}^n \frac{1}{\sqrt{2\pi}\sigma_x} e^{-\frac{(I_{(x)i}-\mu_x)^2}{2\sigma_x^2}} \quad (10)$$

where  $L(\mu_x, \sigma_x^2|H_x)$  is the harmonic likelihood function,  $\mu_x$  and  $\sigma_x^2$  are the two parameters of harmonic positive distribution, and  $e$  is the natural base number of the normal distribution.

The logarithm is taken on both sides of formula (10). The formula is given as follows:

$$\begin{cases} \ln L(\mu_x, \sigma_x^2|H_x) = -\eta_1 - \eta_2 - \eta_3 \\ \eta_1 = \frac{n}{2} \ln(2\pi) \\ \eta_2 = \frac{n}{2} \ln(\sigma_x^2) \\ \eta_3 = \frac{1}{2\sigma_x^2} \sum_{i=1}^n (I_{(x)i} - \mu_x)^2 \end{cases} \quad (11)$$

where  $\eta_1$ ,  $\eta_2$ , and  $\eta_3$  are the polynomials of the logarithmic result of the likelihood function; then, the probability maximum of the harmonic parameter  $\theta_x$  is easily found. The two parameters  $\mu_x$  and  $\sigma_x^2$  of the harmonic normal distribution in formula (11) are derived. The formulae are shown in (12) and (13) [24]

$$\frac{\partial \ln L(\mu_x, \sigma_x^2|H_x)}{\partial \mu_x} = \frac{1}{\sigma_x^2} \sum_{i=1}^n (I_{(x)i} - \mu_x) \quad (12)$$

$$\frac{\partial \ln L(\mu_x, \sigma_x^2|H_x)}{\partial \sigma_x^2} = -\frac{n}{2\sigma_x^2} + \frac{1}{2\sigma_x^2} \sum_{i=1}^n (I_{(x)i} - \mu_x)^2. \quad (13)$$

Combining (12) and (13), the maximum estimates  $\mu_{(x)\text{MLE}}$  and  $\sigma_{(x)\text{MLE}}^2$  of the harmonic normal distribution parameters are obtained. The formulae are shown in (14) and (15) [25]

$$\mu_{(x)\text{MLE}} = \frac{1}{n} \sum_{i=1}^n I_{(x)i} \quad (14)$$

$$\sigma_{(x)\text{MLE}}^2 = \frac{1}{n} \sum_{i=1}^n \left( I_{(x)i} - \left( \frac{1}{n} \sum_{i=1}^n I_{(x)i} \right) \right)^2 \quad (15)$$

where  $\mu_{(x)\text{MLE}}$  and  $\sigma_{(x)\text{MLE}}^2$  are the unique solutions of the harmonic MLE equation and the maximum value of this likelihood equation, respectively. Therefore, the maximum likelihood estimate of the harmonic normal distribution parameter ( $\mu_x$ ,  $\sigma_x^2$ ) is  $(\mu_{(x)\text{MLE}}, \sigma_{(x)\text{MLE}}^2)$ .

The phase and amplitude of harmonics are obtained from the harmonic data of the photovoltaic inverter. Each harmonic datum is composed of a unique amplitude and phase. Formulae (7)–(15) calculate the optimal harmonic amplitude. By utilizing the amplitude of harmonics, the corresponding unique harmonic data of the photovoltaic inverter are matched, and this includes the phase of the harmonics. Therefore, the phase is obtained.

Fig. 2 shows the specific schematic diagram for constructing the harmonic MLE for grid-connected PVs.

In Fig. 2, first, the likelihood function is constructed for the harmonic current with normal distribution characteristics.

In order to avoid overflow under the calculation of the likelihood function, a logarithmic treatment is performed. Furthermore, the two parameters in the likelihood function are derived, and the maximum estimates of the two parameters of the harmonic normal distribution are obtained  $\mu_{(x)\text{MLE}}$  and  $\sigma_{(x)\text{MLE}}^2$ . These provide a basis for the evaluation of the hosting capacity under the influence of harmonics.

#### B. Harmonic Partition

Harmonics are distributed throughout the distribution network according to the direction of the harmonic power flow. In order to

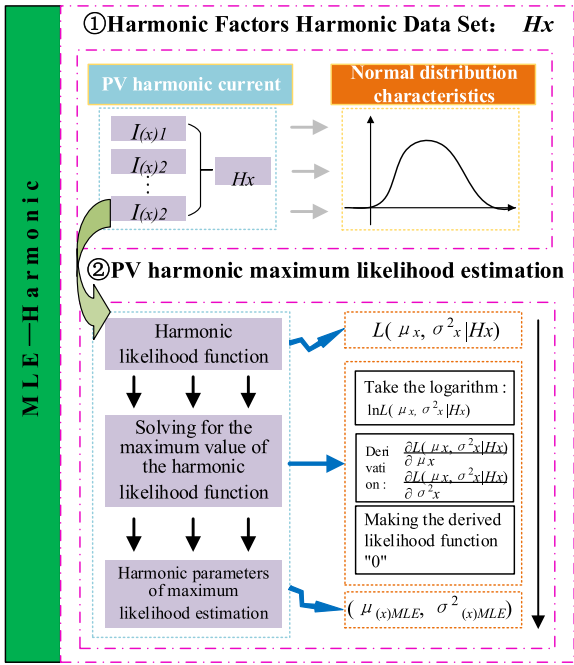


Fig. 2. Schematic diagram of harmonic MLE.

evaluate the hosting capacity in different harmonic regions, the electrical distance can be used to partition the distribution network into distinct regions. The electrical distance is an important index for reflecting the degree of electrical connection between nodes. The electrical distance between node  $i$  and node  $j$  of a distribution network is usually considered to be the sensitivity, which is the variation in load injections at node  $j$  by node  $i$  with respect to voltage variation amplitude  $\Delta U_i$ . The size represents the strength of the connection between nodes. However, the traditional electrical distance is based on the fundamental power flow and the fundamental node admittance matrix. It determines the coupling relationship of each node under fundamental wave conditions, but it fails to capture the connection between nodes under the influence of harmonics, resulting in difficulties when partitioning the distribution network.

Therefore, in the area determination section of the distribution network proposed in this article, a method combining the harmonic admittance matrix and electrical distance is introduced, which divides the distribution network into harmonic regions to enable a more detailed analysis of the hosting capacity in different harmonic regions. First, the harmonic admittance matrix of the distributed photovoltaic grid-connected system is determined using the previously calculated harmonic admittance values. Furthermore, the voltage/reactive power sensitivity matrix of system harmonics is constructed by combining the harmonic admittance matrix with the harmonic partition method based on the improved electrical distance. The degree of connection between photovoltaic grid-connected nodes and other nodes in the distribution network is then analyzed under harmonic conditions. Finally, the harmonic partition of the distribution network is carried out to evaluate the hosting capacity under the influence of harmonics in the region. Fig. 3 shows the schematic diagram of this method.

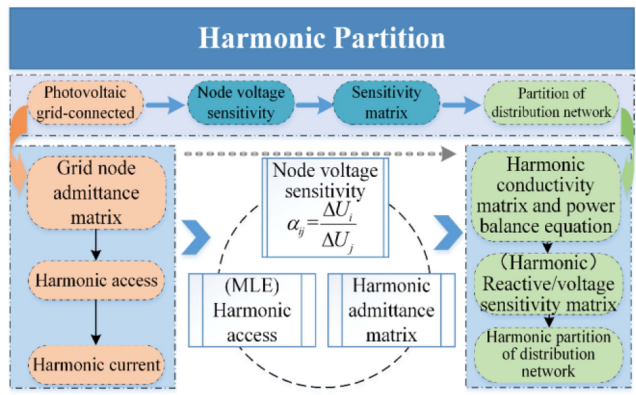


Fig. 3. Schematic diagram of distributed photovoltaic grid-connected harmonic partition.

In Fig. 3,  $\alpha_{ij}$  and  $\alpha_{ji}$  are the sensitivities between nodes  $i$  and  $j$ , and  $\Delta U_i$  and  $\Delta U_j$  are the voltage increments. The construction method based on the harmonic distribution network partition is divided into the following processes.

First, based on the harmonic partition method of the improved electrical distance, the sensitivity between nodes  $i$  and  $j$  is shown as follows:

$$\alpha_{ij} = \frac{\Delta U_i}{\Delta U_j} = \left( \frac{\partial U_i}{\partial Q_j} \right) / \left( \frac{\partial U_j}{\partial Q_j} \right) \quad (16)$$

$$\alpha_{ji} = \frac{\Delta U_j}{\Delta U_i} = \left( \frac{\partial U_j}{\partial Q_i} \right) / \left( \frac{\partial U_i}{\partial Q_i} \right) \quad (17)$$

where  $\alpha_{ij}$  and  $\alpha_{ji}$  are the sensitivities between nodes  $i$  and  $j$ ,  $\Delta U_i$  and  $\Delta U_j$  are the voltage increments, and  $\frac{\partial U_i}{\partial Q_j}$ ,  $\frac{\partial U_j}{\partial Q_j}$ ,  $\frac{\partial U_i}{\partial Q_i}$ , and  $\frac{\partial U_j}{\partial Q_i}$  are the sensitivities of the voltage/reactive power.

From the above, it can be observed that sensitivity is the basis for calculating electrical distances. The voltage/reactive power sensitivity corresponds to the balance equation in Newton–Raphson power flow calculations [26]. The harmonic admittance matrix is used to replace the fundamental admittance matrix in the power balance equation, allowing for the analysis of the sensitivity matrix of voltage/reactive power under harmonic conditions. The polar coordinate power expression of the improved harmonic partition is given as follows:

$$\begin{cases} P_{i,PV} = U_{i,PV} \sum_{j=1}^n U_{j,PV} \\ (G_{(H)ij} \cos \theta_{ij,PV} + B_{(H)ij} \sin \theta_{ij,PV}) \\ Q_{i,PV} = U_{i,PV} \sum_{j=1}^n U_{j,PV} \\ (G_{(H)ij} \sin \theta_{ij,PV} - B_{(H)ij} \cos \theta_{ij,PV}) \end{cases} \quad (18)$$

where  $n$  is the number of distributed photovoltaic grid-connected system nodes, and  $G_{(H)ij}$  and  $B_{(H)ij}$  are the conductance and susceptance of each element in the harmonic admittance matrix, respectively.

Formula (18) is a nonlinear expression, and the matrix of power correction equation is shown as follows [27]:

$$\begin{bmatrix} \Delta P \\ \Delta Q \end{bmatrix} = \begin{bmatrix} \frac{\partial P}{\partial \theta} & \frac{\partial P}{\partial U} \\ \frac{\partial Q}{\partial \theta} & \frac{\partial Q}{\partial U} \end{bmatrix} \begin{bmatrix} \Delta \theta \\ \Delta U \end{bmatrix} = \begin{bmatrix} J_{(H)P\theta} & J_{(H)PU} \\ J_{(H)Q\theta} & J_{(H)QU} \end{bmatrix} \begin{bmatrix} \Delta \theta \\ \Delta U \end{bmatrix} \quad (19)$$

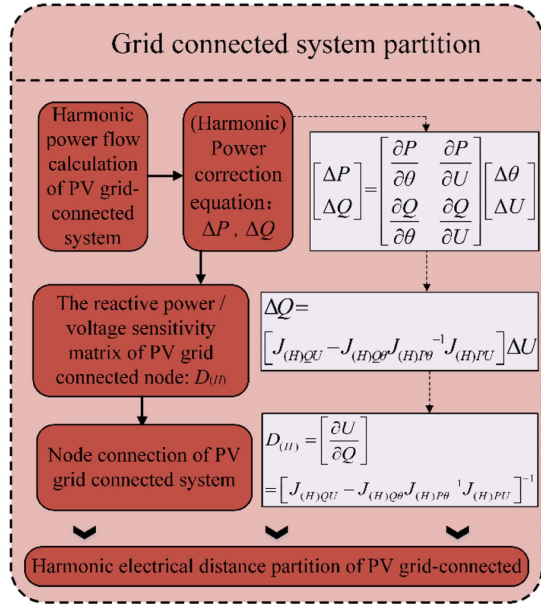


Fig. 4. PV grid-connected partition process diagram.

where  $\Delta P$  and  $\Delta Q$  represent the deviation matrices of active power and reactive power injected by nodes, respectively;  $\Delta \theta$  and  $\Delta U$  represent the change matrices of node voltage phase angle and voltage amplitude, respectively; and  $\frac{\partial P}{\partial \theta}$ ,  $\frac{\partial P}{\partial U}$ ,  $\frac{\partial Q}{\partial \theta}$ , and  $\frac{\partial Q}{\partial U}$  correspond to  $J_{(H)P\theta}$ ,  $J_{(H)PU}$ ,  $J_{(H)Q\theta}$ , and  $J_{(H)QU}$  in the harmonic Jacobian matrix, respectively, which are the partial derivatives between power and node voltages.

Neglecting the effect of  $\Delta P$  on the voltage variation [28], the sensitivity relationship of voltage/reactive power in the harmonic case is shown as follows:

$$\Delta Q = [J_{(H)QU} - J_{(H)Q\theta} J_{(H)P\theta}^{-1} J_{(H)PU}] \Delta U. \quad (20)$$

On the basis of the distributed photovoltaic grid connection, the voltage/reactive power sensitivity matrix of the harmonic electrical distance is shown as follows:

$$D_{(H)} = \left[ \frac{\partial U}{\partial Q} \right] = [J_{(H)QU} - J_{(H)Q\theta} J_{(H)P\theta}^{-1} J_{(H)PU}]^{-1} \quad (21)$$

where  $D_{(H)}$  is the voltage/reactive power sensitivity matrix of the harmonic electrical distance.

The basis of electrical distance partition is the voltage/reactive power sensitivity matrix.  $P, Q, U$ , and  $\theta$  in the fundamental power flow equation are used with respect to voltage/reactive power sensitivity. The voltage/reactive power sensitivity matrix under the harmonic admittance matrix is analyzed via the harmonic electrical distance partition. Therefore, the formulae of  $P, Q, U$ , and  $\theta$  are applied.

Finally,  $D_{(H)}$  is applied to each node of the distributed photovoltaic grid connection to realize the harmonic partition of the grid-connected system. Fig. 4 shows the detailed process diagram of the system partition.

In Fig. 4,  $D_{(H)}$  is the harmonic sensitivity matrix of the PV grid connection. The value of each matrix element represents the coupling relationship between two nodes in the harmonic case.

The smaller the element value, the stronger the node connection. According to the actual situation of the distributed PV grid connection access capacity, the maximum electrical distance between two nodes is taken as the diameter of the distribution network area, and the PV grid-connected node is taken as the first node (pilot node) of the subdivision. The combination of the above constraints, such as sensitivity coefficient, node connectivity, and area diameter, is used to carry out distribution network harmonic zoning, which provides a basis for hosting capacity evaluation in harmonic regions.

### C. Hosting Capacity Assessment for Distributed Photovoltaic Grid Connections Based on the MLE-Harmonics

Based on the above MLE-harmonic, the random characteristics of harmonic access of distributed photovoltaics in grid-connected systems are extracted, and the likelihood function of the photovoltaic output harmonic is constructed. The maximum estimation of harmonic parameters with normal distribution characteristics is carried out, and the harmonic input of distributed photovoltaics in the grid-connected system is described. Then, the calculation of the harmonic power flow with respect to photovoltaic integration into the distribution network is carried out to obtain the direction and distribution of harmonics in the system. Furthermore, a harmonic partitioning method for photovoltaic grid connections is constructed to analyze the hosting capacity of the distribution network in multiple regions under the influence of harmonics.

Based on the above research, Fig. 5 shows the evaluation step of the maximum hosting capacity of distributed photovoltaics integrated into the distribution network.

In Fig. 5, according to the harmonic MLE and harmonic partition method based on the harmonic power flow, the maximum hosting capacity evaluation process of distributed photovoltaics in the distribution network is constructed. First, the likelihood function for the PV output harmonics is established, providing a maximum estimation of harmonic parameters with normal distribution characteristics and depicting the harmonic inputs. Then, the fundamental parameters of the photovoltaic grid-connected system components are transformed into harmonic parameters, and the harmonic node admittance matrix is constructed to calculate the harmonic power flow. Next, a harmonic constraint model is constructed for hosting capacity evaluation, and a more realistic hosting capacity of the distribution network is obtained by comprehensively considering multiple types of constraints. Furthermore, the distribution network is partitioned using the voltage/reactive power sensitivity matrix based on the harmonic admittance matrix, which solves the problem of multiscenario distributed photovoltaic access to the distribution network. Simultaneously, the harmonic partition method reduces calculation times while ensuring the accuracy of photovoltaic capacity access. Combined with the various constraint models mentioned above, a particle swarm optimization algorithm is used to quickly obtain the maximum hosting capacity in a more suitable harmonic region of the distribution network.

In the hosting capacity assessment carried out in this study, regardless of the harmonic variations, the statistical analysis

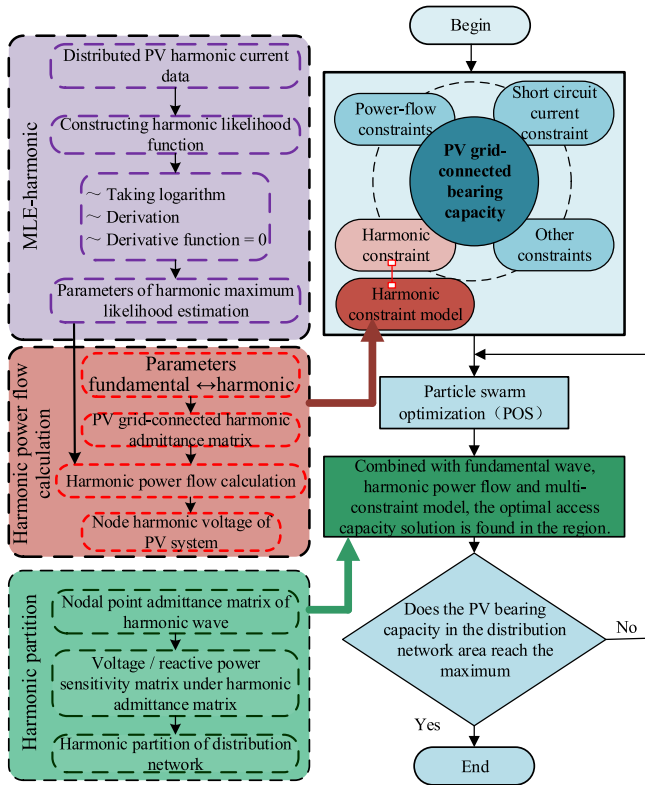


Fig. 5. Process diagram of evaluation of the maximum hosting capacity of PV grid connected.

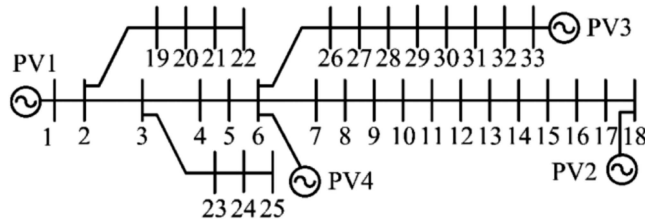


Fig. 6. IEEE-33 node and PV wiring diagram.

methodology adopted by the authors, using harmonic data prior to the PV connection to the network, analyzes the range and characteristics of the harmonic dynamics. By combining the range and characteristics of harmonic data, a harmonic constraint condition was constructed for photovoltaic grid-connected systems, ensuring the scientific and rational evaluation of hosting capacities. Therefore, using MLE for the statistical analysis of harmonic ranges and characteristics is suitable for photovoltaic grid-connected systems.

#### IV. ALGORITHM VERIFICATION

To verify the feasibility and effectiveness of the proposed hosting capacity evaluation method, this study utilizes the IEEE-33 node system, with the feeder used to connect the distributed photovoltaic system, as shown in Fig. 6.

In Fig. 6, the reference voltage is 12.66 kV, the reference capacity is 10 MVA, and PV is the distributed photovoltaic access. The endpoint and middle point of the IEEE-33 system are

selected. Values of 1, 18, 33, and 6 are taken as the first harmonic injection nodes of the system subpartition, which is divided into Region I, Region II, Region III, and Region IV. Furthermore, feeders are used to connect distributed photovoltaics at nodes 1, 18, 33, and 6 to achieve a reasonable partition of the IEEE-33 node; this permits a comprehensive analysis of the hosting capacity under the injection harmonics.

#### A. MLE Analysis Results of Distributed Photovoltaic Grid-Connected Harmonic Output

The harmonic current generated by the distributed photovoltaic system comprises mainly low-order and odd-order harmonics [29]. Therefore, we take the 3rd, 5th, 7th, 9th, and 11th harmonics as an example. According to the harmonic current data generated by distributed photovoltaics, the maximum estimated value of harmonic normal distribution parameters can be obtained using (7)–(15). Here, the equation is given as follows:

$$[\mu_{MLE(h)} \quad \sigma^2_{MLE(h)}] = \begin{bmatrix} 0.07_{(3)} & 0.020^2_{(3)} \\ 0.10_{(5)} & 0.024^2_{(5)} \\ 0.10_{(7)} & 0.023^2_{(7)} \\ 0.05_{(9)} & 0.019^2_{(9)} \\ 0.05_{(11)} & 0.023^2_{(11)} \end{bmatrix} \quad (22)$$

where  $h$  is the number of photovoltaic harmonics ( $h = 3, 5, 7, 9$ , and  $11$ ); and  $\mu_{MLE(h)}$  and  $\sigma^2_{MLE(h)}$  are the maximum estimated values of the harmonic parameter. The normal distribution curve of the main harmonics is obtained. In the harmonic sample of the photovoltaic inverter, there are many different harmonic sample values, and each harmonic sample value is composed of a unique amplitude and phase. In the article, the amplitude of harmonics is estimated via the maximum likelihood value, and the optimal harmonic amplitude is determined. Furthermore, the corresponding harmonic phase is found among the harmonic sample values using the optimal harmonic magnitude. The amplitude and phase of the harmonic are determined as the amount of harmonics injected into the photovoltaic grid-connected system; then, the harmonic vector operation and harmonic power flow calculation are performed.

#### B. Harmonic Partition

According to the grid-connected harmonic admittance in the MLE above, the IEEE-33 system is divided into harmonic partitions. Since the system incorporates four distributed PVs, divided into four regions, the sensitivity matrices of voltage/reactive power are analyzed for each of the four connected PV nodes, as shown in Fig. 7.

In Fig. 7, the vertical coordinate is the voltage/reactive power sensitivity, which represents the coupling relationship between the other nodes and the PV grid-connected nodes in the case of harmonics, and the smaller the value, the stronger the connection between the nodes. In the figure, the red dividing line is the most suitable voltage/reactive power sensitivity critical value. Harmonic partition processing is performed on nodes with distribution network values that are less than the critical value. Fig. 8 shows the partition results.

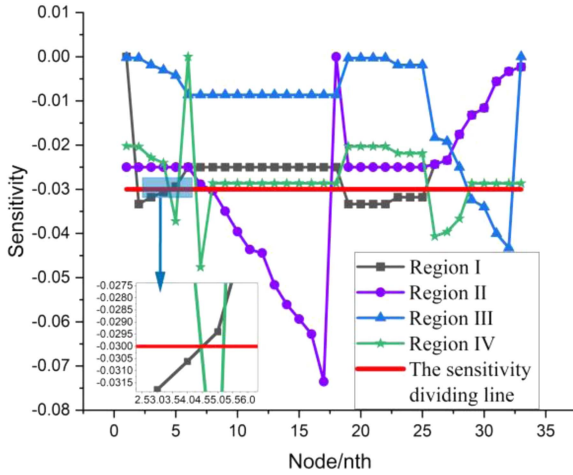


Fig. 7. Voltage/reactive power sensitivity of grid-connected system.

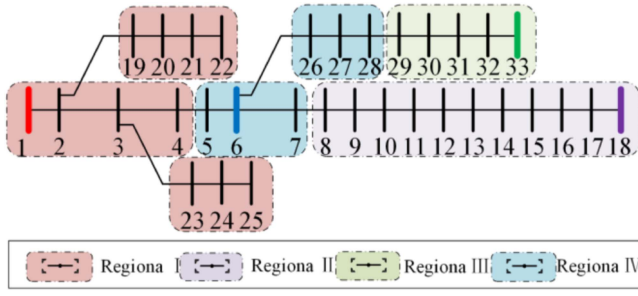


Fig. 8. Results of IEEE-33 system harmonic partition.

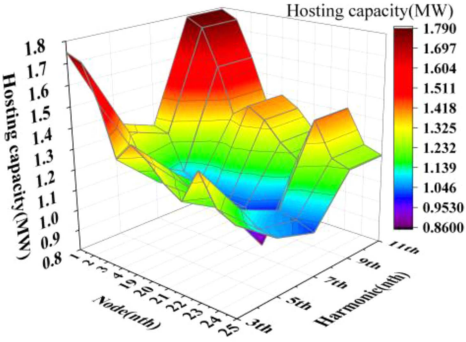


Fig. 9. Region I.

In Fig. 8, the harmonic partition of the distributed photovoltaic grid-connected system is carried out. According to the concept of harmonic partitioning above, the nodes within a harmonic region are strongly coupled and connected. Consequently, the hosting capacity within this region changes significantly during the harmonic injection of PV. The harmonic connection between nodes in different regions is not close, and the influence of the hosting capacity between them is very small. While ensuring the accuracy of PV capacity access, the regional hosting capacity evaluation of the distribution network can be performed quickly.

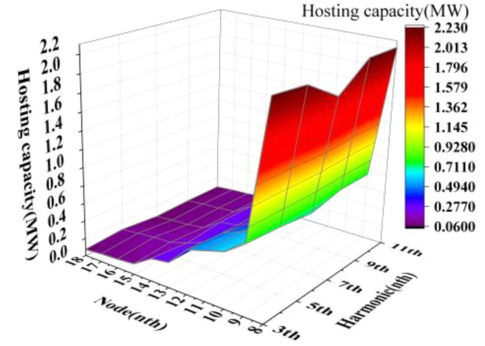


Fig. 10. Region II.

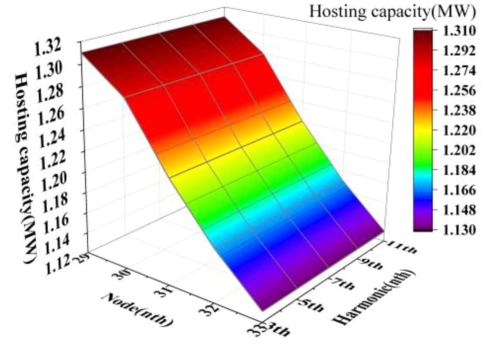


Fig. 11. Region III.

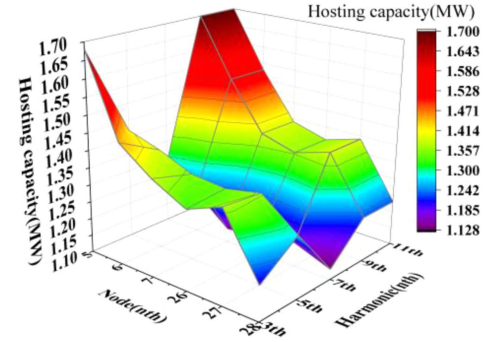


Fig. 12. Region IV.

### C. Maximum Hosting Capacity Assessment Results

Based on the method described in Section III, this study analyzes the maximum hosting capacity in the region for a distributed network with PV using the MLE of each harmonic. Figs. 9–12 show the calculation results.

In Figs. 9–12, the hosting capacity of different regions and harmonic frequencies in the distribution network is evaluated, as observed, with the exception of Region III. The hosting capacity corresponding to the seventh harmonic is relatively less than that corresponding to the other harmonics. This indicates that the seventh harmonic is the dominant harmonic in the data and network topology of the example. The harmonic current is larger, and the harmonic constraints formed are more demanding, which will reduce the maximum hosting capacity of the distribution network. Similarly, other numbers of harmonics, such as the 3rd

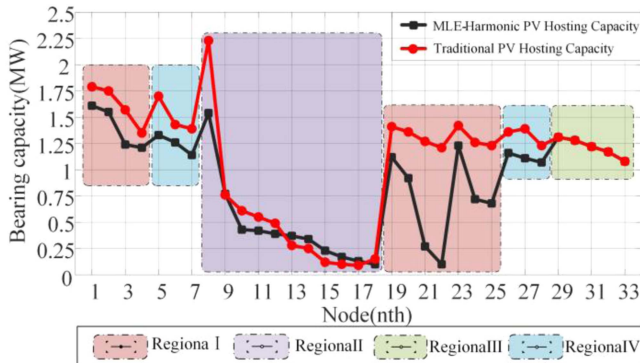


Fig. 13. Comparison of grid-connected hosting capacity of distributed photovoltaics.

and 11th harmonics, which have smaller harmonic currents, cannot constrain the maximum hosting capacity of the distribution network too substantially.

From Fig. 11, it can be observed that, in Region III, the hosting capacity of the distribution network corresponding to each harmonic is consistent. It characterizes the fact that harmonic constraints do not dominate among the multiple hosting capacity constraints. This maximum capacity does not make the harmonic THD exceed the limit; thus, it does not meet the requirements that affect the maximum hosting capacity of the distribution network. Therefore, Region III has the same maximum hosting capacity.

Furthermore, the MLE-harmonic constraint is compared with the traditional nonharmonic constraint in the evaluation results of distribution network's hosting capacity, as shown in Fig. 13.

In Fig. 13, it can be observed that under the MLE-harmonic constraints, the distribution network's hosting capacity in Region I, Region II, and Region IV is relatively low. The hosting capacity in each region has a large floating reduction, and the photovoltaic grid connection has a clearer limit capacity, which ensures the safe operation of the distribution network. Comparing the MLE-harmonic hosting capacity and traditional hosting capacity, it can be observed that, under the MLE-harmonic constraints, the distribution network hosting capacity in Region I, Region II, and Region IV is relatively low. The typical harmonic constraint condition, which is the average harmonic value, results in high bearing capacities and no binding forces. The MLE-harmonic method reduces the hosting capacity in various regions, and the PV grid connection has a clearer limit capacity, ensuring the safe operation of the distribution network. Therefore, the hosting capacity evaluation method based on the harmonic MLE is more aligned with the actual grid-connected system. Consequently, the more realistic maximum hosting capacity is reflected.

Table I lists the statistical data of the maximum hosting capacity assessment. Mode 1 uses the average value of harmonics, a typical harmonic constraint condition, to evaluate the hosting capacity of the PV grid connection. Mode 2 represents the evaluation method of the maximum hosting capacity of the PV grid connection under MLE-harmonic and electrical distance

TABLE I  
STATISTICAL TABLE OF MAXIMUM HOSTING CAPACITY EVALUATION TIME

Mode	Region	Regional time	Cumulative time
(Mode 1) Average harmonic value	\	\	>2700 s
(Mode2) MLE-harmonic	Region I	261 s	873 s
	Region II	279 s	
	Region III	149 s	
	Region IV	101 s	

partitions, which reduced calculation times. Therefore, the strategy proposed in this study can effectively reduce the evaluation time of the maximum hosting capacity of the distributed PV grid connection.

The results for the example show that the harmonic partitioning method proposed in this study can quickly evaluate the local hosting capacity of the distribution network while ensuring the accuracy of photovoltaic capacity access, further reducing calculation times. It is evident that this method can comprehensively consider multiple constraints, such as harmonics, allowing for the maximum hosting capacity evaluation of distributed photovoltaic grid connections. The method's superiority with respect to calculation accuracy and efficiency is demonstrated, ensuring the safe operation of the grid-connected system. Therefore, this method is deemed reasonable.

## V. CONCLUSION

A novel hosting capacity evaluation method for distributed PV connection in power systems based on the MLE-harmonic system is proposed herein. The methodology accounts for the harmonics generated by distributed PV grid connections, and the harmonic quantities of PV grid connections are characterized using MLE-harmonics. This enables a more realistic estimation of the maximum hosting capacity for PV grid connections. In addition, based on the improved electrical distance, the voltage/reactive power sensitivity under the harmonic admittance matrix is constructed, dividing the PV grid-connected system into harmonic regions. The maximum hosting capacity is then evaluated within these regions. Harmonic partitioning addresses the issues of multiple scenarios and long calculation times in traditional maximum hosting capacity analysis. Validation through examples demonstrated that the method proposed in this article provides a more reliable reference for hosting capacities in distribution networks with PV and ensures the safe operation of the distribution network.

## REFERENCES

- [1] X. Yu et al., "Distributed photovoltaic installation admittance optimization: An end-to-end approach," *IEEE Trans. Smart Grid*, vol. 14, no. 6, pp. 4942–4952, Nov. 2023.

- [2] M. A. Khan, A. Haque, V. S. B. Kurukuru, and S. Mekhilef, "Advanced control strategy with voltage sag classification for single-phase grid-connected photovoltaic system," *IEEE J. Emerg. Sel. Topics Ind. Electron.*, vol. 3, no. 2, pp. 258–269, Apr. 2022.
- [3] M. Deakin et al., "Hybrid open points: An efficient tool for increasing network capacity in distribution systems," *IEEE Trans. Power Del.*, vol. 37, no. 2, pp. 1340–1343, Apr. 2022.
- [4] Y. Zhu, J. Yang, and Q. D Zhang, "Planning of distributed generation based on optimal real power losses," *Power Syst. Protection Control*, vol. 39, no. 21, pp. 12–16, 2011.
- [5] S. Wang, Y. Dong, L. Wu, and B. Yan, "Interval overvoltage risk based PV hosting capacity evaluation considering PV and load uncertainties," *IEEE Trans. Smart Grid*, vol. 11, no. 3, pp. 2709–2721, May 2020.
- [6] M. Mahdavi, K. E. K. Schmitt, and F. Jurado, "Robust distribution network reconfiguration in the presence of distributed generation under uncertainty in demand and load variations," *IEEE Trans. Power Del.*, vol. 38, no. 5, pp. 3480–3495, Oct. 2023.
- [7] G. Yang et al., "Implications of future price trends and interannual resource uncertainty on firm solar power delivery with photovoltaic overbuilding and battery storage," *IEEE Trans. Sustain. Energy*, vol. 14, no. 4, pp. 2036–2048, Oct. 2023.
- [8] A. Askarzadeh, "A memory-based genetic algorithm for optimization of power generation in a microgrid," *IEEE Trans. Sustain. Energy*, vol. 9, no. 3, pp. 1081–1089, Jul. 2018.
- [9] S. M. Arif, A. Hussain, T. T. Lie, S. M. Ahsan, and H. A. Khan, "Analytical hybrid particle swarm optimization algorithm for optimal siting and sizing of distributed generation in smart grid," *J. Modern Power Syst. Clean Energy*, vol. 8, no. 6, pp. 1221–1230, 2020.
- [10] F. Ahmadi-Gorjayi and H. Mohsenian-Rad, "A physics-aware MIQP approach to harmonic state estimation in low-observable power distribution systems using harmonic phasor measurement units," *IEEE Trans. Smart Grid*, vol. 14, no. 3, pp. 2111–2124, May 2023.
- [11] I. Sarantakos, N.-M. Zografou-Barredo, D. Huo, and D. Greenwood, "A reliability-based method to quantify the capacity value of soft open points in distribution networks," *IEEE Trans. Power Syst.*, vol. 36, no. 6, pp. 5032–5043, Nov. 2021.
- [12] A. Ahmad, H. D. Tafti, G. Konstantinou, B. Hredzak, and J. E. Fletcher, "Distributed photovoltaic inverters' response to voltage phase-angle jump," *IEEE J. Photovolt.*, vol. 12, no. 1, pp. 429–436, Jan. 2022.
- [13] J. K. M. Becker et al., "Modelling of AC/DC interactions of converter-interfaced resources for harmonic power-flow studies in microgrids," *IEEE Trans. Smart Grid*, vol. 14, no. 3, pp. 2096–2110, May 2023.
- [14] M. Sharifzadeh, H. Vahedi, R. Portillo, L. G. Franquelo, and K. Al-Haddad, "Selective harmonic mitigation based self-elimination of triplen harmonics for single-phase five-level inverters," *IEEE Trans. Power Electron.*, vol. 34, no. 1, pp. 86–96, Jan. 2019.
- [15] Y. Zhang et al., "Charging and discharging strategies of independent energy storage for distribution grid side considering distributed PV carrying capacity," *Electr. Power*, vol. 57, no. 4, pp. 111–117, 2024.
- [16] A. Argüello, R. Torquato, B. Rosado, and W. Freitas, "Modeling of single-phase photovoltaic generators for system-wide harmonic power flow studies," *IEEE Trans. Energy Convers.*, vol. 38, no. 2, pp. 914–926, Jun. 2023.
- [17] B. Gao, Y. Wang, and W. Xu, "Modeling voltage source converters for harmonic power flow studies," *IEEE Trans. Power Del.*, vol. 36, no. 6, pp. 3426–3437, Dec. 2021.
- [18] W. Zhou, O. Ardakanian, H.-T. Zhang, and Y. Yuan, "Bayesian learning-based harmonic state estimation in distribution systems with smart meter and DPMU data," *IEEE Trans. Smart Grid*, vol. 11, no. 1, pp. 832–845, Jan. 2020.
- [19] Y. Lian, S. Yang, H. Ben, W. Bai, and W. Yang, "A parallel-connected 24-pulse rectifier using hybrid harmonic reduction method at DC side," *IEEE Trans. Power Electron.*, vol. 37, no. 11, pp. 12932–12937, Nov. 2022.
- [20] S. C. Surace and J.-P. Pfister, "Online maximum-likelihood estimation of the parameters of partially observed diffusion processes," *IEEE Trans. Autom. Control*, vol. 64, no. 7, pp. 2814–2829, Jul. 2019.
- [21] Y. Baghzouz and O. Tan, "Probabilistic modeling of power system harmonics," *IEEE Trans. Ind. Appl.*, vol. IA-23, no. 1, pp. 173–180, Jan. 1987.
- [22] M.-W. Wu, Y. Jin, Y. Li, T. Song, and P.-Y. Kam, "Maximum-likelihood, magnitude-based, amplitude and noise variance estimation," *IEEE Signal Process. Lett.*, vol. 28, no. 4, pp. 414–418, Jan. 2021.
- [23] C.-H. Wu, T.-R. Tsai, and M.-Y. Lee, "Two-stage maximum likelihood estimation procedure for parallel constant-stress accelerated degradation tests," *IEEE Trans. Rel.*, vol. 70, no. 2, pp. 446–458, Jun. 2021.
- [24] Y. Xu et al., "RSSI-based direction of arrival estimation using maximum likelihood estimator and UHF antenna array," in *Proc. IEEE Int. Conf. High Voltage Eng. Appl.*, 2020, pp. 1–4.
- [25] N. Zhou, L. Luo, H. Song, G. Sheng, and X. Jiang, "A substation UHF partial discharge directional of arrival estimation method based on maximum likelihood estimation," in *Proc. IEEE Conf. Elect. Insul. Dielectr. Phenomena*, 2019, pp. 279–282.
- [26] H. Bao and G. Fang, "A new method of electrical distance calculation and its applications used the equivalent transmission impedance method," *Power Syst. Technol.*, vol. 43, no. 1, pp. 244–250, 2019.
- [27] H. Cui, F. Li, and X. Fang, "Effective parallelism for equation and Jacobian evaluation in large-scale power flow calculation," *IEEE Trans. Power Syst.*, vol. 36, no. 5, pp. 4872–4875, Sep. 2021.
- [28] L. Lu, G. Geng, Y. Ji, X. Li, and Z. Wei, "Voltage control partitioning method for active distribution network based on electrical distance matrix eigenvalue analysis," *Electr. Power Construction*, vol. 39, no. 1, 2018, Art. no. 83.
- [29] N. Xie et al., "Dynamic modeling and characteristic analysis on harmonics of photovoltaic power stations," *Proc. CSEE*, vol. 33, no. 36, pp. 10–17, 2013.